BJP British Journal of Pharmacology

DOI:10.1111/bph.12068
www.brjpharmacol.org

RESEARCH PAPER

Enhanced anti-tumour effects of Vinca alkaloids given separately from cytostatic therapies

H Ehrhardt[1,2], L Pannert[1], S Pfeiffer[1], F Wachter[1], E Amtmann[3] and I Jeremias[1,4]

[1]*Helmholtz Zentrum München, German Research Center for Environmental Health, Munich, Germany,* [2]*Division of Neonatology, University Children's Hospital, Perinatal Center, Ludwig-Maximilians-University Munich, Munich, Germany,* [3]*German Cancer Research Centre, Heidelberg, Germany, and* [4]*Department of Oncology/Hematology, Dr. von Haunersches Kinderspital, München, Germany*

Correspondence
Irmela Jeremias, Helmholtz Center Munich, German Research Center for Environmental Health, Marchioninistrasse 25, D-81377 München, Germany. E-mail: irmela.jeremias@helmholtz-muenchen.de

Keywords
doxorubicin; vincristine; p53; cell cycle arrest; application schedule

Received
26 June 2012
Revised
29 September 2012
Accepted
22 October 2012

BACKGROUND AND PURPOSE

In polychemotherapy protocols, that is for treatment of neuroblastoma and Ewing sarcoma, Vinca alkaloids and cell cycle-arresting drugs are usually administered on the same day. Here we studied whether this combination enables the optimal antitumour effects of Vinca alkaloids to be manifested.

EXPERIMENTAL APPROACH

Vinca alkaloids were tested in a preclinical mouse model *in vivo* and *in vitro* in combination with cell cycle-arresting drugs. Signalling pathways were characterized using RNA interference.

KEY RESULTS

In vitro, knockdown of cyclins significantly inhibited vincristine-induced cell death indicating, in accordance with previous findings, Vinca alkaloids require active cell cycling and M-phase transition for induction of cell death. In contrast, anthracyclines, irradiation and dexamethasone arrested the cell cycle and acted like cytostatic drugs. The combination of Vinca alkaloids with cytostatic therapeutics resulted in diminished cell death in 31 of 36 (86%) tumour cell lines. In a preclinical tumour model, anthracyclines significantly inhibited the antitumour effect of Vinca alkaloids *in vivo*. Antitumour effects of Vinca alkaloids in the presence of cytostatic drugs were restored by caffeine, which maintained active cell cycling, or by knockdown of p53, which prevented drug-induced cell cycle arrest. Therapeutically most important, optimal antitumour effects were obtained *in vivo* upon separating the application of Vinca alkaloids from cytostatic therapeutics.

CONCLUSION AND IMPLICATIONS

Clinical trials are required to prove whether Vinca alkaloids act more efficiently in cancer patients if they are applied uncoupled from cytostatic therapies. On a conceptual level, our data suggest the implementation of polychemotherapy protocols based on molecular mechanisms of drug–drug interactions.

LINKED ARTICLE

This article is commented on by Solary, pp 1555–1557 of this issue. To view this commentary visit http://dx.doi.org/10.1111/bph.12101

Abbreviations

doxo, doxorubicin; FP, fractional product; VCR, vincristine

Introduction

To increase antitumour efficacy, chemotherapy is always given as polychemotherapy; several drugs are applied together, usually within a few hours (Frei, 1985; Dy and Adjei, 2008). The reason for combining certain drugs, but not others, derives from empirical studies (Frei, 1985; Ramaswamy, 2007; Dy and Adjei, 2008). Unfortunately, detailed

systematic optimization of drug combinations in clinical trials has not been possible due to limited resources (Benz *et al.*, 2007; Bendall, 2011).

Furthermore, a basic understanding of the mechanisms of the mode of action of chemotherapeutic drugs has not been fully elucidated. In fact, the interaction between two or more drugs is rarely unravelled on a molecular level, which has meant that, so far, the choice of favourable drug combinations is not based on a mechanistic understanding of their interactions (Bonadonna *et al.*, 1995; 2004; Kaspers *et al.*, 1995; Ling *et al.*, 1996; Müller and Boos, 1998; Akutsu *et al.*, 2002; Barone *et al.*, 2007; Benz *et al.*, 2007; Li *et al.*, 2007; Mayer and Janoff, 2007; Bendall, 2011).

For example, it is questionable whether drugs that arrest the cell cycle should be combined with drugs that require active cell cycling for their effect (Rixe and Fojo, 2007; Ewald *et al.*, 2010). In the case of Vinca alkaloids, if cell cycling and M transition are disabled, they are unable to induce cell death in tumour cells (Kawamura *et al.*, 1996; Ewald *et al.*, 2010; Ehrhardt *et al.*, 2011a).

Cell cycle arrest represents a hallmark of chemotherapy. For many cytotoxic drugs, cell cycle arrest is an important mechanism of action, and one of the most prominent features of several classes of cytotoxic drugs is their ability to induce cell cycle arrest (Rixe and Fojo, 2007; Ewald *et al.*, 2010). Drugs that induce cell cycle arrest are known as cytostatic drugs (Rixe and Fojo, 2007; Ewald *et al.*, 2010). In the intracellular signal transduction pathway, these cytostatic drugs activate p53, which mediates both cell cycle arrest and cell death (Resnick-Silverman and Manfredi, 2006; Suzuki and Matsubara, 2011). Anthracyclines as well as γ-irradiation and dexamethasone are all known to induce cell cycle arrest (Jänicke *et al.*, 2001; Mattern *et al.*, 2007; Ehrhardt *et al.*, 2011a).

In polychemotherapeutic protocols for the treatment of solid tumours such as neuroblastoma, nephroblastoma, Ewing sarcoma and multiple myeloma, Vinca alkaloids are given on the same day as cytostatic drugs such as anthracyclines and γ-irradiation. Here we investigated whether this combination allows the optimal antitumour effects of Vinca alkaloids to be elicited. In a recent study on acute leukaemia cells, we showed that combining anthracyclines with Vinca alkaloids significantly reduced their antitumour effects as compared with separate applications (Bendall, 2011; Ehrhardt *et al.*, 2011a). Here we investigated whether this negative interaction also occurs in solid tumour cells, which signalling steps are responsible for it and, most importantly, how Vinca alkaloids should be applied for maximum efficacy in cancer patients.

Methods

Materials

The following antibodies were used: anti-Bcl-xL, anti-caspase-2, anti-cleaved Casp-3, anti-cleaved Casp-6, anti-cleaved Casp-7, anti-cleaved PARP, anti-cyclin B and anti-p-Histone H3 Ser^{10} from Cell Signaling Technology (Danvers, MA); anti-Bcl-2, anti-Histone H1 and anti-p53 from Santa Cruz (Santa Cruz, CA); anti-α-tubulin from Oncogene (San Diego, CA); anti-Casp-9 from Transduction Laboratories (San Diego, CA); anti Casp-10 from MBL (Watertown, MA); anti-cyclin D1 from BD Biosciences (San Jose, CA) and anti-caspase-8 from Alexis Corp (Lausen, Switzerland). Caffeine, vincristine, mimosine, pifithrine-α and L-thymidine were obtained from Calbiochem (Darmstadt, Germany). All other reagents were obtained from Sigma (St. Louis, MO).

Cell lines, transfection experiments and primary samples

All cell lines were obtained from DSMZ (Braunschweig, Germany) and maintained as previously described (Ehrhardt *et al.*, 2003; Baader *et al.*, 2005). HCT 116 $p53^{-/-}$ and $p53^{+/+}$ were a kind gift of B Vogelstein (Bunz *et al.*, 1998). For cell line experiments, cells were seeded at 0.05×10^6 mL^{-1} and incubated with chemotherapeutic drugs at peak plasma concentration for 48 h unless otherwise stated.

Transfection experiments where performed using Lipofectamine for SHEP cells for stable transfection and Lipofectamine 2000 (Invitrogen Corporation, Carlsbad, CA) for the transient transfection of A498 and stable transfection of Calu6 cells according to the manufacturers' instructions; for the transfection of shRNAs against the different cyclins, lentiviral transfection was applied (Ehrhardt *et al.*, 2011b; 2012). shRNA p53, shcyclinA and corresponding mock plasmids were as previously described (Ehrhardt *et al.*, 2008; 2011a,b; 2012). For the generation of pGreen Puro constructs containing shRNAs targeting cyclin B or cyclin D1 oligonucleotides targeting 3′-CTTTACATGGGAGGTCTTTAA-5′ or 3′-GTTTG TCTAGTAGGCGTTT-5′ were annealed (Yuan *et al.*, 2006).

Animal trial

All studies involving animals are reported in accordance with the ARRIVE guidelines for reporting experiments involving animals (Kilkenny *et al.*, 2010; McGrath *et al.*, 2010). The animal trials were approved by the Baden-Württemberg federal government, and animal care was in accordance with institution's guidelines. Female mice aged 8–12 weeks of the Swiss Nu/Nu strain were obtained from Charles River (Sulzfeld, Germany). Animals were kept in fully conditioned rooms at 22°C ± 1°C temperature, humidity 55% ± 10%, regular day / night rhythm of 12/12 h, regular cage changes and food *at libitum*. A total of 100 mice was used for the experiments. The mice were injected s.c. with 0.1 mL cell solution (corresponding to 5×10^6 cells) in the right flank. After 14 days, all animals had developed tumours with diameters ranging between 6 and 11 mm. The animals were distributed into groups of 10 animals each and treated with i.p. injections of doxorubicin solution (0.15 $mg \cdot mL^{-1}$; Farmitalia, Freiburg, Germany) and/or vincristine solution (0.05 $mg \cdot mL^{-1}$, i.v.; Medac, Hamburg, Germany). The tumour size (two dimensions) was determined at the beginning of treatment and was followed for 15 days. The relative change in tumour size was determined for each animal.

Cell imaging, apoptosis assays and Western blot analysis

Cell death was measured using Nicoletti staining for solid tumour cells and forward side scatter analysis for leukaemia cells. In addition, in selected experiments the Annexin V/PI-double staining was performed in parallel to verify the accuracy of the techniques (Nicoletti *et al.*, 1991; Ehrhardt *et al.*,

2011a). For biochemical inhibition, cell lines were pretreated for 6 h or for irradiated experiments 24 h before further stimulation. Cell cycle analysis and detection of cyclin D1 or p-Histone H3 Ser^{10} was performed using the recently described technique of combining intracellular specific antibody and PI staining (Ehrhardt *et al.*, 2011a). Western blot analysis of total cellular protein or of cytosolic and nuclear fractions was performed as previously described (Ehrhardt *et al.*, 2008; 2012).

Statistical analysis

Specific apoptosis was calculated as [(apoptosis of stimulated cells at end minus apoptosis of unstimulated cells at end) divided by (100 minus apoptosis of unstimulated cells at end) ×100]; specific survival was calculated as [100-specific apoptosis induction]. Fractional product method (FP) was employed as described. FP-values ≤ –0.1 were defined as relevant antagonism; FP values ≥ 0.1 as relevant synergism (Webb, 1963). Dose–effect curves were performed by CompuSyn software version 1.0.

In Figure 3F, doxorubicin resistance was defined as specific apoptosis of less than 10%. All cell line data are presented as the mean values of at least three independent experiments ± SEM, unless otherwise stated. To test for significant differences, Student's paired *t*-test was applied; for multivariate analysis, one way RM ANOVA was used. Significance was set at $P < 0.05$. For the animal trials, Student's *t*-test was applied, with differences considered significant when $P < 0.01$.

Results

Vincristine requires active cell cycling for induction of cell death

Vinca alkaloids are known to induce cell death in tumour cells by inhibiting the assembly of microtubule structures and disrupting mitosis in the metaphase (Kawamura *et al.*, 1996; Mollinedo and Gajate, 2003). Accordingly, Vinca alkaloids require active cell cycling of target cells for induction of cell death.

For our studies, we used SHEP neuroblastoma cells as patients with neuroblastoma receive Vinca alkaloids and anthracyclines on the same day; the results obtained using these SHEP cells are depicted in Figures 1–6. To confirm these results, the experiments were repeated in a second, unrelated cell line, A498 renal cell carcinoma cells; the results obtained with these A498 cells are shown in Supporting Information Figure S5. Comparable *in vitro* data were also obtained in CALU-6 lung cancer and MCF-7 breast cancer cells, to extend the phenotype described to further tumour entities (data not shown).

In SHEP neuroblastoma tumour cells, knockdown of cyclin B, which arrested the cell cycle in G2 phase, largely prevented the cell death induced by vincristine (VCR) (Figure 1A). In parallel, the knockdown of cyclin A arrested cells in the G2 phase and also reduced cell death induced by VCR (Figure 1B and C). The negative effect of cell cycle arrest was not restricted to arrest in the G2 phase. To extend the studies to other phases of the cell cycle, a further knockdown strategy and biochemical cell cycle arrest were implemented. To arrest the tumour cells in the G1 phase, the specific knockdown of cyclin D1 was selected, which – as published previously – led to an incomplete but statistically significant arrest in G1 without interference with the basal apoptosis rate of transfected cells (Figure 1B; Klier *et al.*, 2008; Anastasov *et al.*, 2009). The cell cycle arrest in the G1 phase significantly inhibited VCR-induced cell death (Figure 1C). Similarly, biochemical cell cycle arrest in the G0 phase induced by depriving the cells of serum (starvation), in the G1 phase by L-mimosine or in the G2 phase by L-thymidine attenuated the apoptosis induced by VCR (Figure 1D and Table 1). On a molecular level, these data reproduce the known fact that VCR requires active cell cycling of target cells for induction of cell death. Taken together, the inhibitory effect of cell cycle arrest on the activity of VCR was observed for the three different cell cycle checkpoints studied and for molecular and biochemical settings of cell cycle arrest: arrest in G0, G1 and G2. The results confirm that active cell cycling and the progression from G2 to the M phase are critical for VCR efficacy; VCR exerts its cytotoxic effect by arresting the cells in the M phase.

Table 1

Cell cycle distribution in SHEP cells after biochemical cell cycle inhibition

Cell cycle distribution	G0	G1	G2	M
Control	3.0%	71.9%	17.9%	3.6%
0% FCS	34.5%	58.5%	4.2%	0.3%
Mimosine	1.1%	87.4%	9.3%	0.6%
L-thymidine	1.2%	60.8%	34.6%	0.2%

SHEP cells were treated by withdrawal of FCS (0%FCS), with mimosine (100 μM) or L-thymidine (300 μM) as in Figure 1D. Cell cycle distribution was performed using PI staining as in Figure 1A. cyclin D1 was used to discriminate G0 and G1 phases, p-Histone-H3 to separate arrest in G2 and M phase. The resulting cell cycle distribution is presented.

Several antitumour therapeutics arrest the cell cycle

In addition to cytotoxic drugs that induce cell death in target tumour cells, several anti-cancer therapeutics act like cytostatic drugs arresting the cell cycle and inhibiting tumour growth. Among these, anthracyclines like doxorubicine (doxo) and γ-irradiation arrest the cell cycle in the G2 phase, while dexamethasone arrests the cell cycle in the G1 phase (Figure 2) (Jänicke *et al.*, 2001; Mattern *et al.*, 2007; Ehrhardt *et al.*, 2011a).

Cytostatic therapeutics reduce the antitumour effects of Vinca alkaloids

So far, we have reproduced the known facts that Vinca alkaloids require active cell cycling for induction of cell death in tumour cells, and that anthracyclines, γ-irradiation and dexamethasone arrest the cell cycle. In theory, one might conclude that a concomitant combination of both therapeutics appears undesirable.

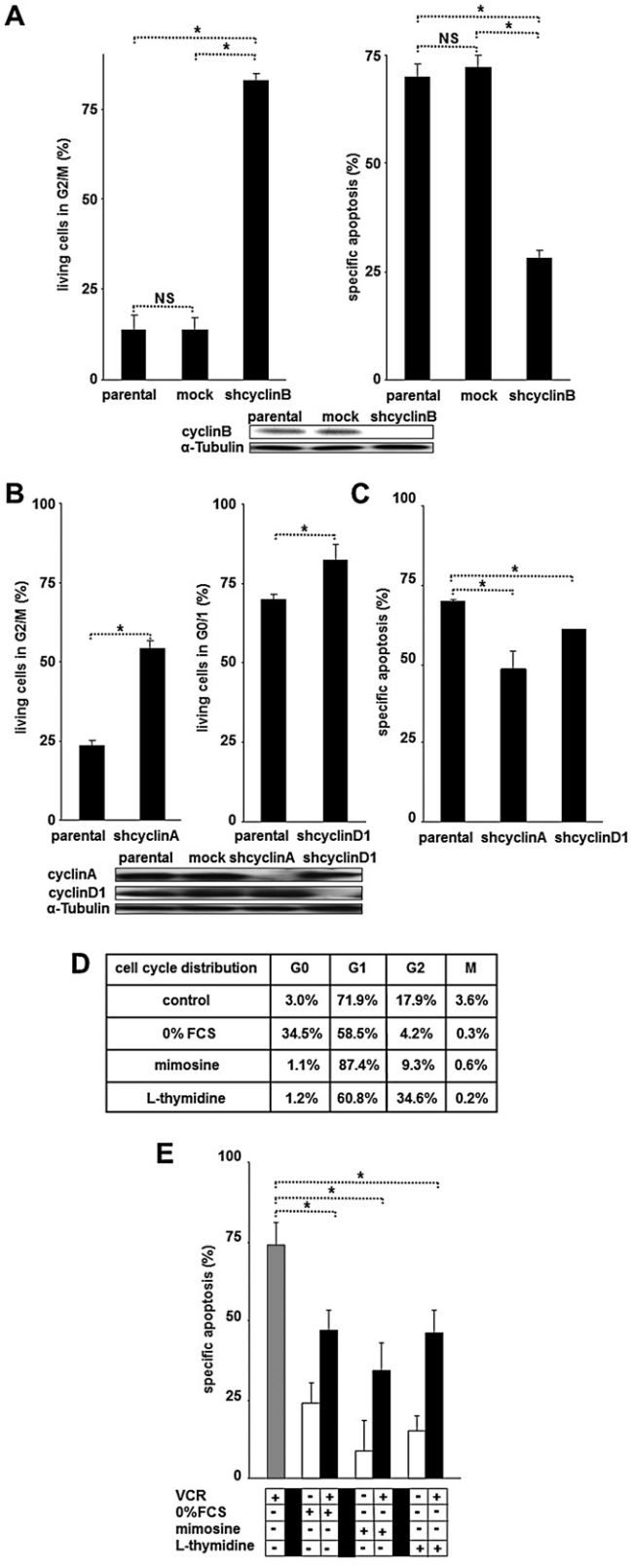

cell cycle distribution	G0	G1	G2	M
control	3.0%	71.9%	17.9%	3.6%
0% FCS	34.5%	58.5%	4.2%	0.3%
mimosine	1.1%	87.4%	9.3%	0.6%
L-thymidine	1.2%	60.8%	34.6%	0.2%

Figure 1

Negative interaction between cell cycle arrest and Vinca alkaloids induced apoptosis. (A) SHEP neuroblastoma cells were stably transfected with a shRNA targeting cyclinB (shcyclinB) or a control mock sequence and were analysed for cell cycle distribution using PI staining (left panel) or apoptosis induction after VCR for 48 h (right panel). (B,C) Parental SHEP cells transiently transfected with shRNA targeting cyclin A or D1 were analysed as in (A). (D) SHEP cells were pretreated by withdrawal of FCS (0%FCS), with mimosine (100 μM) or L-thymidine (300 μM) for 48 h and consecutively stimulated with VCR as in (A). For all cell line experiments, apoptosis was determined by PI staining of fragmented DNA and FACscan analysis, and data are presented as mean ± SEM of at least three independent experiments, if not stated differently. Statistical analysis of cell line data was performed using ANOVA, $*P < 0.05$. NS = not significant.

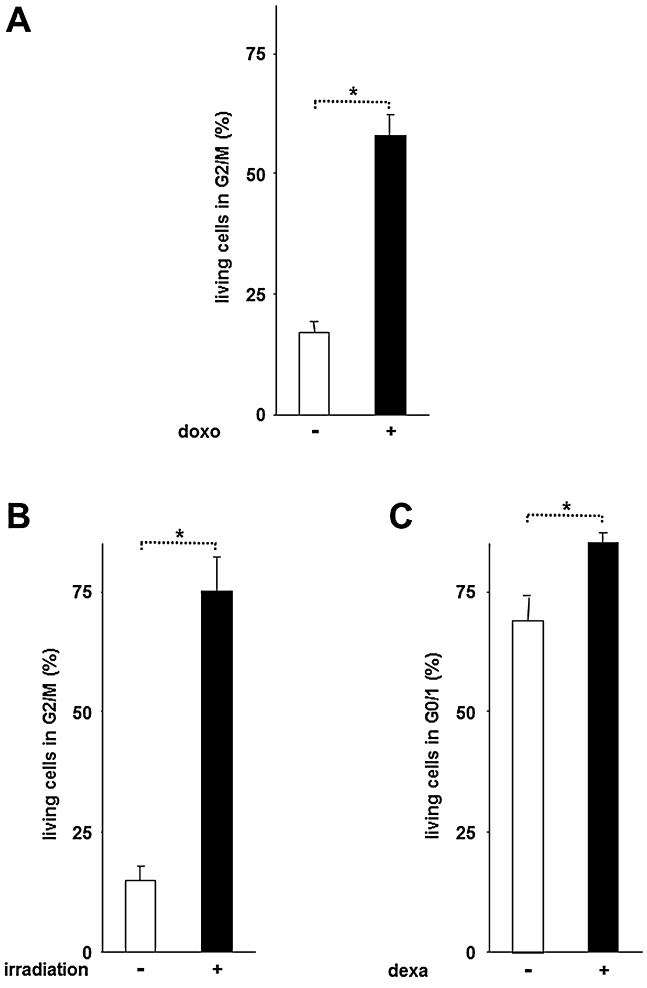

Figure 2

Cell cycle arrest by doxo, irradiation in G2 and dexamethasone (dexa) in G1 in SHEP cells. (A–C) SHEP cells were stimulated with doxo (A, 100 ng·mL^{-1}), irradiated (B, 30Gy) or incubated with dexa (C, 10^{-5}M) for 24 h. Cell cycle analysis was performed, and data presented and analysed as in Figure 1.

To prove this hypothesis, *in vitro* experiments revealed that γ-irradiation, dexamethasone and doxo significantly reduced the antitumour effect of VCR (Figure 3A). More detailed studies were performed on anthracyclines. Dose–effect curves indicated the negative interaction between doxo and VCR over a broad range of clinically relevant drug concentrations in SHEP and Calu6 cancer cells (Figure 3B and C). The negative interaction was further confirmed by the appli-

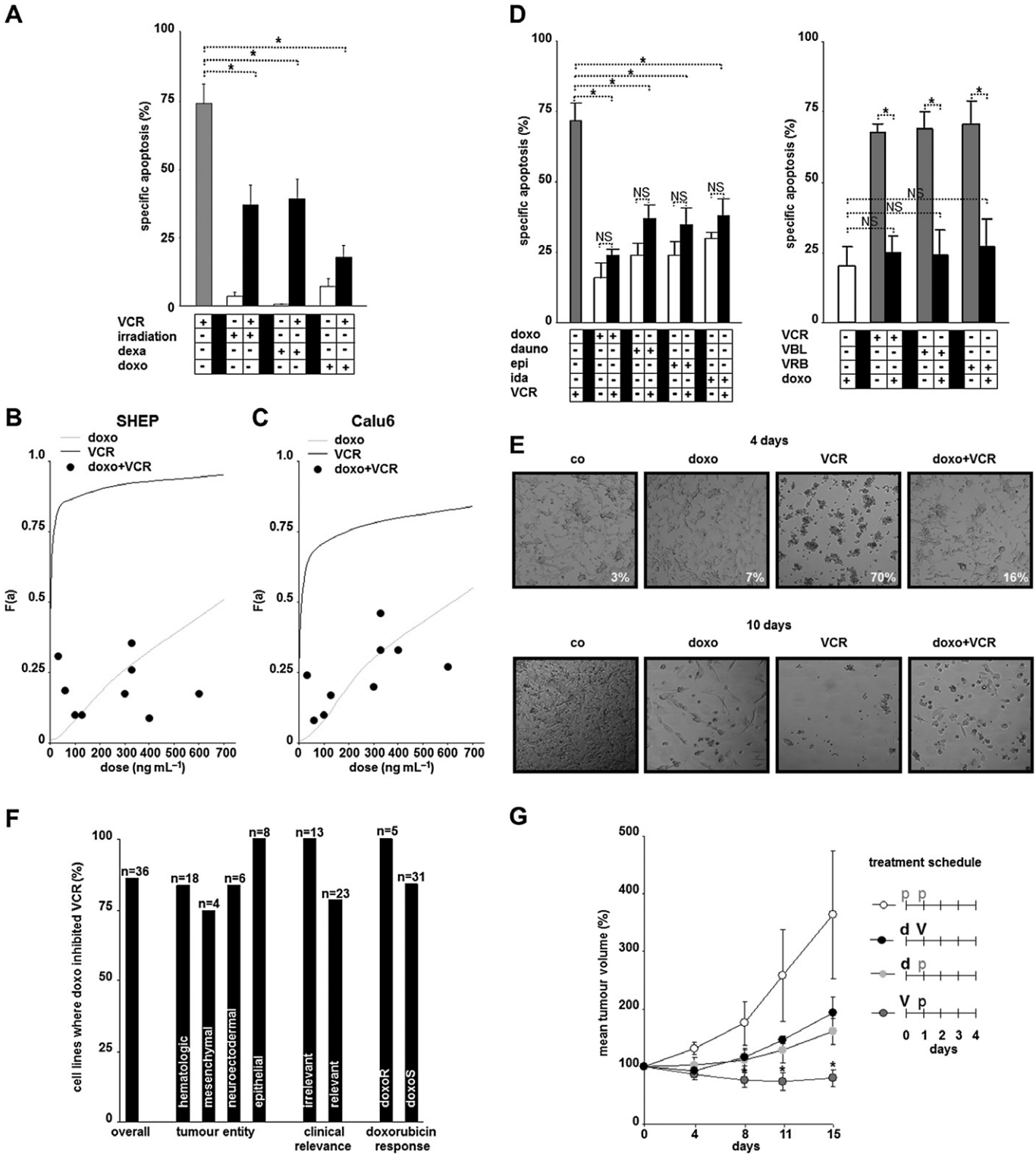

cation of other algorithms like median effect blots or the fractional product method (data not shown). The negative interaction persisted for prolonged periods of time and doxo acted like a classical cell death inhibitor showing a dose-dependent inhibitory function (Supporting Information Figure S1A and B).

Several different anthracyclines, daunorubicin, epirubicin and idarubicin, were also found to inhibit the cell death induced by VCR and doxo inhibited cell death induced by Vinca alkaloids vinblastine and vinorelbine, indicating a general inhibitory effect of members of these two classes of antitumour drugs (Figure 3D). The doxo inhibitory effect on VCR-induced cell death was followed by enhanced colony growth of the tumour cells treated with the combination of the two drugs, which points towards a long-term negative effect beyond direct cytotoxicity (Figure 3E).

Figure 3

Interference of cytostatic drugs with Vinca alkaloid-induced apoptosis. (A) SHEP cells from Figure 2 were additionally treated with VCR as indicated. (B,C) SHEP (B) or Calu-6 lung cancer (C) cells were simultaneously stimulated with doxorubicin (doxo; 30, 100 or 300 ng·mL^{-1}) and vincristine (VCR; 3, 30 or 300 ng·mL^{-1}) as indicated for 48 h. Dose–effect curves were obtained to test for the negative interaction between doxo and VCR. (D) SHEP cells were stimulated with VCR and doxo, daunorubicin (dauno, 100 ng·mL^{-1}), epirubicin (epi, 100 ng·mL^{-1}) or idarubicin (ida, 100 ng·mL^{-1}) (left panel) or with doxo and VCR, vinblastine (VBL, 300 ng·mL^{-1}) or vinorelbine (VRB, 300 ng·mL^{-1}) (right panel) as in (A). (E) Light microscopy pictures of SHEP cells stimulated with doxo (100 ng·mL^{-1}) and VCR (300 ng·mL^{-1}) after 96 h for cell morphology (upper panel) and after 10 days for colony formation (lower panel). Numbers indicate simultaneously determined specific apoptosis. (F) n = 36 tumour cell lines of different origin were stimulated simultaneously with doxo and VCR as in (A) using doxo at 100 ng·mL^{-1} and VCR at 300 ng·mL^{-1} and calculation of the fractional product was performed as described in Methods. Depicted is the fraction of cell lines in which doxorubicin significantly inhibited VCR-induced apoptosis (detailed apoptosis data for solid tumour cell lines are depicted in Supporting Information Figure S1C–E). Data for haematopoietic tumour cells have been published in detail elsewhere (Ehrhardt *et al.*, 2011a). The cell lines were sub-classified by three criteria: (i) by tumour entities as indicated; (ii) by clinical relevance (for tumour entities, where both drugs are applied simultaneously in the clinic, the drug combination was considered as 'relevant', in B- and T-ALL, AML, lymphoma, Ewing's sarcoma and neuroblastoma; otherwise, it was considered 'irrelevant'); and (iii) by sensitivity towards doxorubicin-induced apoptosis ('doxoR' indicates that <10% specific apoptosis was induced by doxo; otherwise, cells were classified as 'doxoS'). n indicates number of cell lines tested. (G) The xenograft study of CALU-6 tumour cells was performed as described in detail in Methods. Animals (10 per group) were treated with vehicle (placebo), doxo (d; 1.5 mg·kg^{-1}) or VCR (V; 0.5 kg^{-1}) alone or doxo followed by VCR 24 h later as indicated in the treatment schedule. Tumour size was measured in two dimensions, and tumour volume was calculated thereof. *P < 0.01, t-test comparing VCR to doxo or the combined application. For all cell line experiments, apoptosis was determined by PI staining of fragmented DNA and FACscan analysis besides leukaemia cell lines (Ehrhardt *et al.*, 2011a), and data are presented as mean ± SEM of at least three independent experiments if not stated differently. Statistical analysis of cell line data was performed using ANOVA, *P < 0.05.

To evaluate the frequency of the inhibitory interaction across the tumour entities, 36 cell lines of various different tumour cell types were screened *in vitro* using doxo and VCR (Supporting Information Figure S1C–E). The fractional product was calculated as described previously (Webb, 1963; Ehrhardt *et al.*, 2011a). In 86% (31/36) of these cell lines and across all tumour types, doxo inhibited the antitumour effect of VCR (Figure 3F, Supporting Information Figure S1C–E). Doxo inhibited VCR in 15 out of 18 (83%) haematological, 3 out of 4 (75%) mesenchymal, 5 out of 6 (83%) neuroectodermal and 8 out of 8 (100%) epithelial tumour cell lines.

In most, but not all, polychemotherapy protocols anthracyclines are given on the same day as Vinca alkaloids. Of the cell lines we tested, twenty-three were derived from tumours, including neuroblastoma and Ewing's sarcoma, that are currently treated clinically by the simultaneous application of Vinca alkaloids and anthracyclines. Of these cell lines, 78% (18 of 23) showed inferior responses if doxo and VCR were combined. All the cell lines resistant to doxo-induced cell death showed a negative interaction, suggesting that anthracycline resistance might predispose tumour cells to the inhibitory effect on VCR (Figure 3F).

To test the interaction of both drugs within the complex *in vivo* situation, mice were xenografted s.c. with human CALU-6 lung carcinoma cells. CALU-6 cells bearing mice were treated with doxo or VCR or both drugs. Similar to the *in vitro* data, doxo significantly inhibited the antitumour effect of VCR *in vivo*, when doxo was applied together with VCR (Figure 3G).

Taken together, doxo frequently and markedly inhibited the antitumour effect of VCR *in vitro* across the majority of tumour types tested and in a preclinical model *in vivo*. Doxo inhibited VCR in tumour entities that are routinely treated with this drug combination in current polychemotherapy protocols in patients.

Signalling mechanism responsible for the negative effect of doxo on VCR-induced cell death

To characterize the mechanism mediating the negative interaction between doxo and VCR, cell cycle analyses were performed. Both doxo and VCR arrested the cell cycle in G2/M, when given alone (Figure 4A). While VCR alone induced cell cycle in M, doxo alone did not (Figure 4B). Treatment with the combination of doxo and VCR resulted in nearly no cells in the M phase (Figure 4B), suggesting that the predominant doxo-induced arrest in G2 prevented the M-phase transition (Ehrhardt *et al.*, 2011a). Furthermore, the combination of doxo and VCR induced a prolonged cell cycle arrest in G2/M compared with the single agents (Figure 4C).

In solid tumour cells, doxo inhibited the identical downstream signalling pathways of VCR-induced apoptosis that we have recently described in leukaemia cells (Ehrhardt *et al.*, 2011a). Phosphorylation of anti-apoptotic Bcl-2 and Bcl-XL was inhibited, which is a pre-condition for their degradation and VCR-induced apoptosis (Supporting Information Figure S2A). Subsequent VCR-induced mitochondrial pore formation, release of cytochrome C and activation of executioner caspases, cleavage of PARP and DNA fragmentation were markedly reduced by doxo (Supporting Information Figure S2B and data not shown). Doxo, VCR or the combination of both did not affect the expression level of the Bcl-2 and IAP family members that represent important antagonists of apoptosis signal transduction (Supporting Information Figure S2C). However, the exception was survivin, which was up-regulated by VCR; this is thought to be an epiphenomenon as overexpression of survivin did not influence the apoptosis response to doxo, VCR or the combination and did not affect the cell cycle distribution (Supporting Information Figure S2D and E).

Taken together, these results indicate that doxo-induced G2 arrest disabled M-phase transition, stabilized anti-apoptotic Bcl-2 family members and inhibited the execution phase of intrinsic apoptosis signalling otherwise induced by VCR.

Restoring the antitumour effects of VCR by preventing p53 accumulation or cell cycle arrest

In patients, each drug should be used at maximum antitumour potency. We next searched for approaches to prevent inhibition of VCR's antitumour effects.

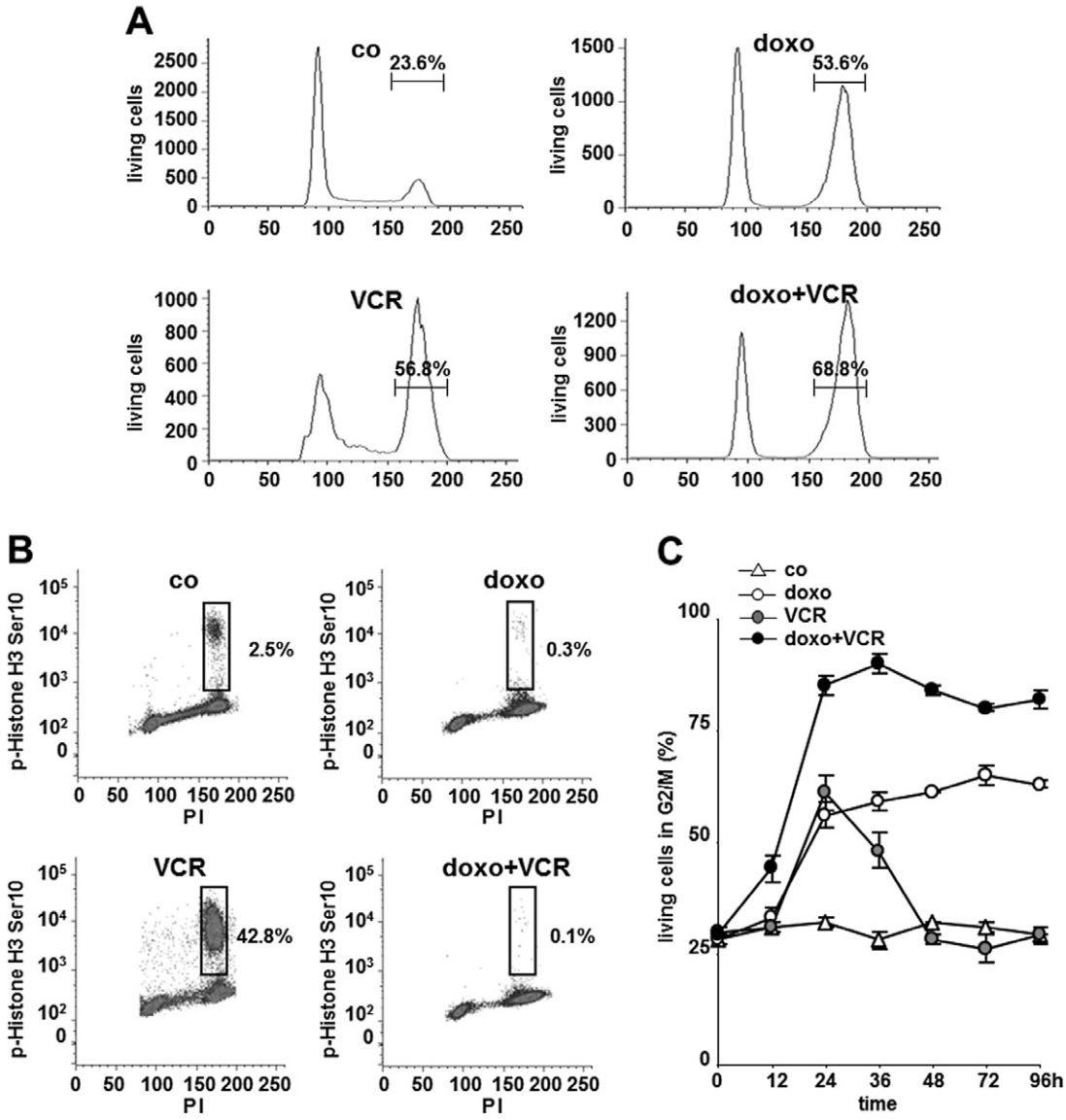

Figure 4

Inhibition of M-phase transition by doxorubicin. (A,B) SHEP cells were stimulated with doxo and VCR for 24 h. Cell cycle analysis was performed using PI staining (A), to discriminate G2 and M arrest, double staining for phospho-Histone H3 (Ser^{10}) and PI was performed (B). PI was measured in the PE-channel, phospho-Histone-H3-Alexa Fluor 488 in the FITC channel of the LSR II. (C) SHEP cells were stimulated with doxo and VCR and cell cycle analysis performed as in (A and B) after incubation times indicated. Data are presented as mean ± SEM of at least three independent experiments.

Figure 5

Therapeutic options to overcome the negative interaction between anthracyclines and Vinca alkaloids mediated by cell cycle arrest. (A) Western blot of nuclear extracts was performed from SHEP cells stimulated with doxo and VCR as in Figure 3A. Histone H1 served as a loading control. (B) SHEP cells were pretreated with pifithrine-α (10 μM) for 6 h followed by stimulation with doxo and VCR. (C) Parental SHEP cells stably transfected with shRNA targeting p53 (shp53) or a control mock shRNA sequence were stimulated with doxo and VCR as in Figure 3A and analysed for cell cycle distribution (left panel, 24 h incubation) or cell death induction (right panel, 48 h incubation). (D) SHEP cells were pretreated with caffeine (300 $\mu g \cdot mL^{-1}$) for 6 h followed by stimulation with doxo and VCR and analysed as in in (C). For all cell line experiments, the concentrations of doxo and VCR, measurement of apoptosis, Western Blot, presentation of data and statistical analysis were performed as described in Figures 1–4.

Within its pleiotropic functions, p53 is known to mediate cell cycle arrest, and all the cell lines studied express functionally active p53 (Zhou and Elledge, 2000; Yu and Zhang, 2005; Petitjean *et al.*, 2007; Rozan and El-Deiry, 2007). That is, doxo induced marked nuclear accumulation of p53, which was unchanged by VCR (Figure 5A and data not shown).

When activation of p53 by doxo was inhibited using the biochemical p53 inhibitor pifithrine-α or knockdown of p53,

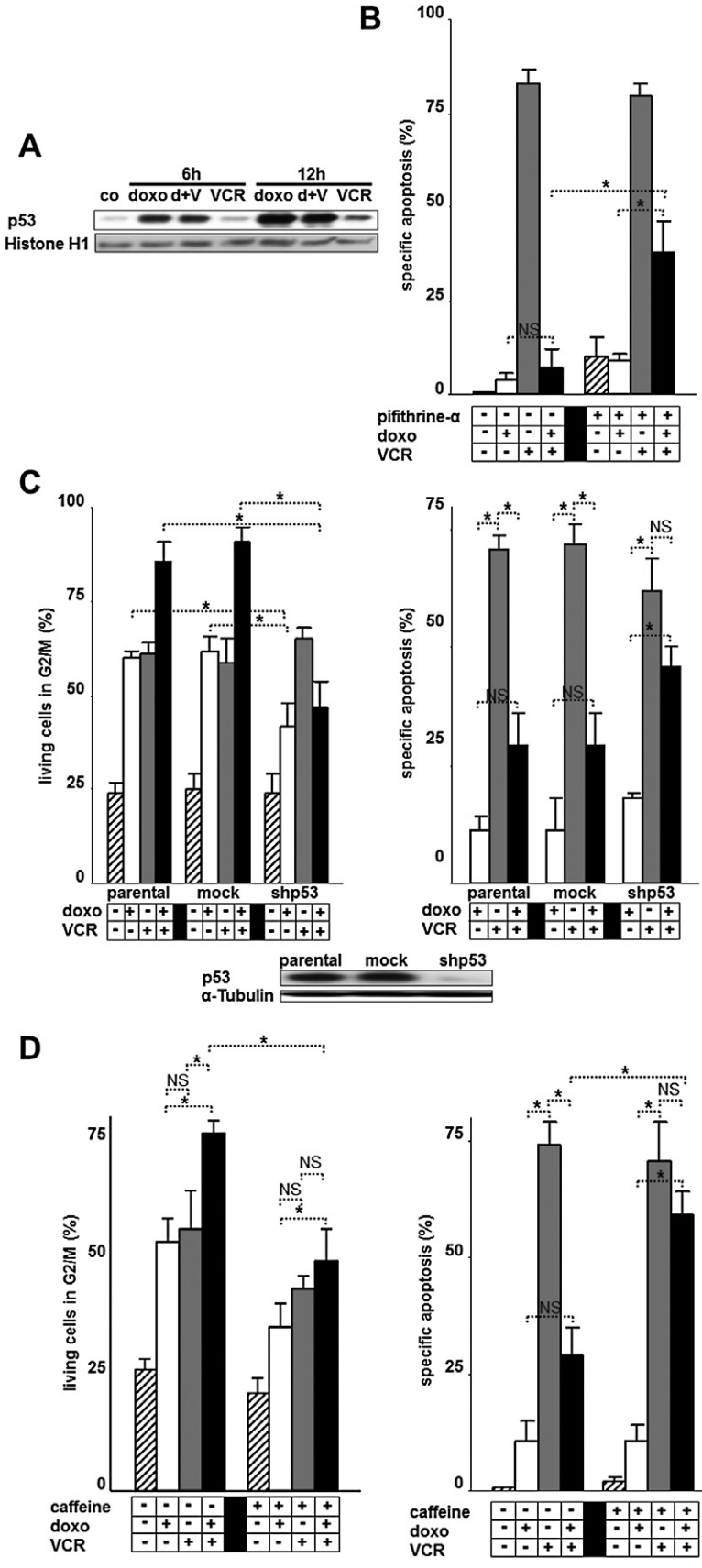
A
6h
12h
co doxo d+V VCR doxo d+V VCR
p53
Histone H1
B
specific apoptosis (%)
100
75
50
25
0
NS
pifithrine-α
doxo
VCR
C
living cells in G2/M (%)
specific apoptosis (%)
parental mock shp53
doxo
VCR
p53
α-Tubulin
D
living cells in G2/M (%)
specific apoptosis (%)
caffeine
doxo
VCR

doxo was unable to induce cell cycle arrest in G2; as a consequence, VCR was able to induce cell death even in the presence of doxo (Figure 5B and C, Supporting Information Figure S3). Knockdown of p53 restored VCR-induced apoptosis in the presence of doxo. These data suggest that doxo requires p53 signalling to arrest the cell cycle and to inhibit VCR-induced cell death. Doxo-induced cell cycle arrest is thus responsible for inhibiting the antitumour effect of VCR. Translated into a clinical context, prevention of p53 accumulation might therefore allow VCR-induced apoptosis in the presence of cytostatic drugs.

Downstream of p53, cell cycle arrest in G2 is the critical signalling step that inhibits VCR-induced apoptosis. For proof of principle and to prevent cell cycle arrest by doxo, cells were pretreated with caffeine. Caffeine alleviated the doxo-induced block in G2 and thereby promoted VCR-induced cell death (Figure 5D). Thus, the negative action of doxo on VCR can be overcome by the addition of a third agent preventing cell cycle arrest (Figure 5D).

Restoring antitumour effects of VCR by preventing cell cycle arrest

As the loss of p53 in HCT116 cells was accompanied by a reduction in the activity of VCR (Supporting Information Figure S3), we studied a far simpler and straightforward translatable approach, the effect of a time-scheduled application of both drugs to prevent the negative interaction between doxo and VCR. Indeed, application of VCR at least 1 or 2 days before doxo enabled VCR to be effective at inducing cell death *in vitro* (Figure 6A). Here, VCR had induced cell death before doxo arrested the cell cycle in target tumour cells. In contrast, when doxo was applied first it disabled the effect of VCR.

To further elucidate the sequence dependency of both drugs within the complex *in vivo* situation, a second independent preclinical trial was performed using the mouse model of xenografted human CALU-6 lung carcinoma cells. Mice bearing CALU-6 cells were treated with doxo or VCR using different application schedules. A time-delayed application of doxo after VCR was included. Similar to the *in vitro* data, VCR exerted its complete antitumour effect, if doxo was applied after, but not before or together with VCR (Figure 6B). When VCR was given first, VCR induced cell death in M phase before doxo arrested cells in G2. Thus, both drugs act most efficiently, when given separately from each other. The antitumour efficacy of treatment with doxo and VCR was highly dependent on the sequence of application. In an additional independent animal trial, animals treated with VCR alone lived longer than animals treated with the combination of doxo and VCR, showing that the addition of doxo to VCR reduced the survival time of the mice (Supporting Information Figure S4; Ehrhardt *et al.*, 2011a).

Taken together and within polychemotherapy protocols, VCR acts most effectively, if it is applied uncoupled from cytostatic drugs; this allows VCR to act on actively cycling tumour cells, not cells in cell cycle arrest.

The present results suggest that the negative action of doxo on VCR can be overcome by a novel application schedule, which is easily translatable into clinical polychemotherapy protocols. Our data propose the use of old drugs in

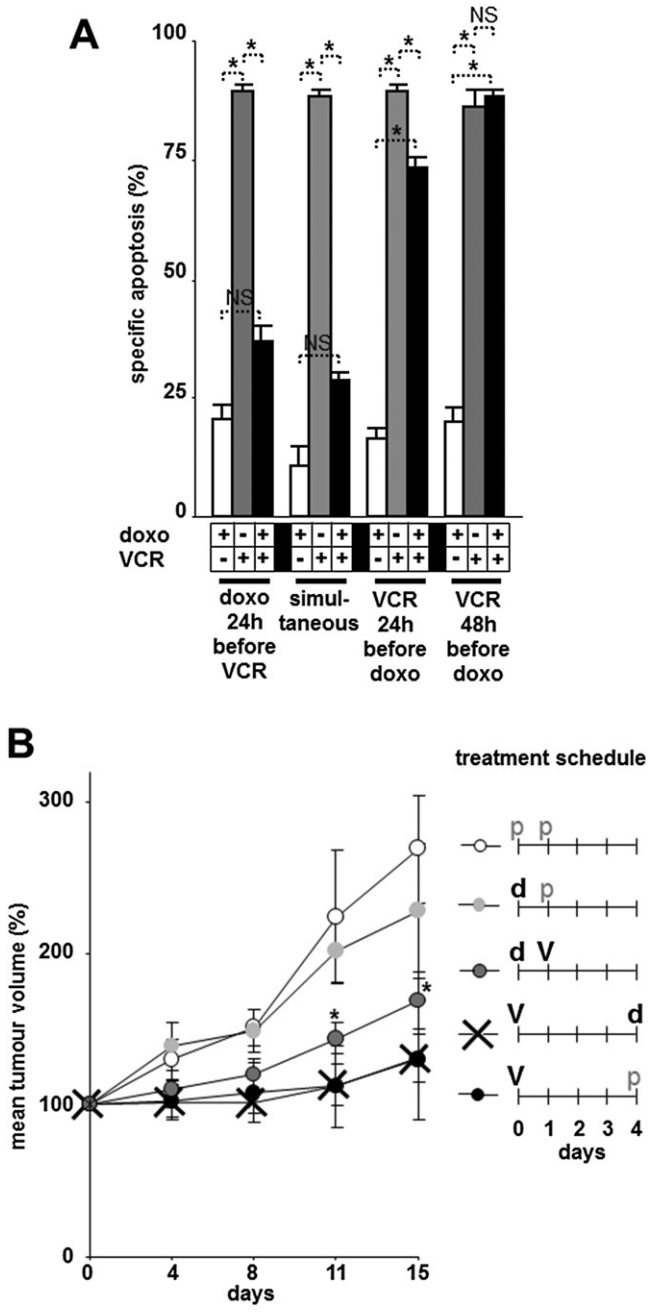

Figure 6

Facilitation of maximum antitumour efficiency by sequential application of vincristine before doxorubicin. (A) SHEP cells were stimulated with doxorubicin (doxo, 100 ng·mL^{-1}) and vincristine (VCR, 300 ng·mL^{-1}) with application intervals indicated. Apoptosis was measured 48 h after addition of the second drug. *$P < 0.05$, ANOVA. NS = not significant, h = hour. (B) Xenograft study of CALU-6 tumour cells implanted s.c. into nude mice was performed as described in Methods and in Figure 3G. Mice were treated once with doxo (d; 0.3 mg·kg^{-1}) and/or VCR (V; 0.1 mg·kg^{-1}) or placebo as depicted. Tumour size was measured in two dimensions, and tumour volume was calculated. Statistical analysis revealed that doxo followed by VCR 1 day later significantly inhibited the effect of VCR alone (*$P < 0.01$, *t*-test), whereas VCR followed by doxo 4 days later did not differ from VCR alone. For the cell line experiment, the concentrations of doxo and VCR, measurement of apoptosis, presentation of data and statistical analysis were performed as described in Figures 1 and 3.

new, optimized application schedules with the aim of increasing the antitumour efficacy of Vinca alkaloids in cancer patients.

Discussion and conclusions

Our *in vivo* and *in vitro* data show that Vinca alkaloids exert their maximum antitumour effects on solid tumour cells, when given separately from cytostatic drugs. As an underlying mechanism, Vinca alkaloids require active cell cycling for the induction of cell death, while cytostatic drugs arrest the cell cycle thereby inhibiting Vinca alkaloids. Based on the molecular understanding of the interaction of these classes of drugs, maximum antitumour effects of Vinca alkaloids in combination with cytostatic drugs were achieved by (i) inhibiting cell cycle arrest by blockade of p53, (ii) by addition of substances that promote cell cycling or (iii) by separate application of the two drugs a few days apart.

Recently, we have described the antagonistic effect of anthracyclines on the actions of Vinca alkaloids on leukaemia cells (Ehrhardt *et al.*, 2011a). We demonstrated here for the first time (i) that in solid tumour cells the antitumour effectiveness of Vinca alkaloids is highest when they are applied separately from cytostatic drugs; (ii) using RNA interference, we proved that the cell cycle was the important signalling step, where both signalling pathways converge; (iii) in a preclinical mouse model, we showed that separate application of both drugs restored full antitumour activity of VCR. These new data clearly demonstrate the general significance of the presented mechanism for all kinds of tumour entities.

Vinca alkaloids are not the only cytotoxic drugs requiring active cell cycling for induction of cell death in tumour cells; several classes of cytotoxic drugs and γ-irradiation induce cell cycle arrest (Jänicke *et al.*, 2001; Mattern *et al.*, 2007; Rixe and Fojo, 2007; Ewald *et al.*, 2010; Ehrhardt *et al.*, 2011a). Similar to the combination of Vinca alkaloids and anthracyclines, cytotoxic and cytostatic drugs are frequently combined in current polychemotherapy protocols (Jänicke *et al.*, 2001; Mattern *et al.*, 2007; Rixe and Fojo, 2007; Ewald *et al.*, 2010; Bendall, 2011; Ehrhardt *et al.*, 2011a). On a more general level, the data presented suggest the premise that cytotoxic and cytostatic drugs are most effective at inducing antitumour effects, when given on the same day in polychemotherapy, should be re-evaluated. Further research is needed to evaluate preclinically whether further drug combinations act more efficiently upon separate application compared with simultaneous application, in a similar way as shown here for anthracyclines and Vinca alkaloids.

On a broader level, the vision of targeted therapies might be expanded towards targeted drug combinations. Here, the signalling pathway activated by each drug should be characterized and the interplay of both pathways identified. A molecular understanding of underlying signalling mechanisms of drugs and drug combinations will enable a major conceptional change in the design of future polychemotherapy protocols for cancer patients: molecular, preclinical studies might reveal promising, targeted, candidate drug combinations and application schedules for clinical trials.

Acknowledgements

HE, LP, SP and FW performed experiments. EA performed the animal trial. HE and IJ designed the research, provided administrative support, analysed and interpreted the data, prepared the figures and wrote the paper.

The survivin expression plasmid was a kind gift from D Altieri. The plasmid containing shRNA against cyclin B was a kind gift from K Strebhardt.

This work was supported by Dr Helmut Legerlotz Stiftung and Bettina Bräu Stiftung (all to IJ).

Conflicts of interest

There are no other personal financial holdings of any of the authors that could be perceived as constituting a potential conflict of interest. None of the authors has any past or present financial links, including consultancies with manufacturers of material or devices, described in the paper as well as links to the pharmaceutical industry or regulatory agencies or any other potential conflicts of interest.

References

Akutsu M, Furukawa Y, Tsunoda S, Izumi T, Ohmine K, Kano Y (2002). Schedule-dependent synergism and antagonism between methotrexate and cytarabine against leukemia cell lines in vitro. Leukemia 16: 1808–1817.

Anastasov N, Klier M, Koch I, Angermeier D, Höfler H, Fend F *et al.* (2009). Efficient shRNA delivery into B and T lymphoma cells using lentiviral vector-mediated transfer. J Hematop 2: 9–19.

Baader E, Toloczko A, Fuchs U, Schmid I, Beltinger C, Ehrhardt H *et al.* (2005). TRAIL-mediated proliferation of tumor cells with receptor-close apoptosis defects. Cancer Res 65: 7888–7895.

Barone C, Landriscina M, Quirino M, Basso M, Pozzo C, Schinzari G *et al.* (2007). Schedule-dependent activity of 5-fluorouracil and irinotecan combination in the treatment of human colorectal cancer: in vitro evidence and a phase I dose-escalating clinical trial. Br J Cancer 96: 21–28.

Bendall LJ (2011). It's all in the timing. Blood 118: 5983–5984.

Benz EJ Jr, Nathan DG, Amaravadi RK, Danial NN (2007). Targeting the cell death-survival equation. Clin Cancer Res 13: 7250–7253.

Bonadonna G, Zambetti M, Valagussa P (1995). Sequential or alternating doxorubicin and CMF regimens in breast cancer with more than three positive nodes. Ten-year results. JAMA 273: 542–547.

Bonadonna G, Zambetti M, Moliterni A, Gianni L, Valagussa P (2004). Clinical relevance of different sequencing of doxorubicin and cyclophosphamide, methotrexate, and Fluorouracil in operable breast cancer. J Clin Oncol 22: 1614–1620.

Bunz F, Dutriaux A, Lengauer C, Waldman T, Zhou S, Brown JP *et al.* (1998). Requirement for p53 and p21 to sustain G2 arrest after DNA damage. Science 282: 1497–1501.

Dy GK, Adjei AA (2008). Systemic cancer therapy: evolution over the last 60 years. Cancer 113: 1857–1887.

Ehrhardt H, Fulda S, Schmid I, Hiscott J, Debatin KM, Jeremias I (2003). TRAIL induced survival and proliferation in cancer cells resistant towards TRAIL-induced apoptosis mediated by NFκB. Oncogene 22: 3842–3852.

Ehrhardt H, Haecker S, Wittmann S, Maurer M, Borkhardt A, Toloczko A *et al.* (2008). Cytotoxic drug-induced, p53-mediated upregulation of Caspase-8 in tumor cells. Oncogene 27: 783–793.

Ehrhardt H, Schrembs D, Moritz C, Wachter F, Haldar S, Graubner U *et al.* (2011a). Optimized anti-tumor effects of anthracyclines plus vinca alkaloids using a novel, mechanism-based application schedule. Blood 118: 6123–6131.

Ehrhardt H, Wachter F, Maurer M, Stahnke K, Jeremias I (2011b). Important role of Caspase-8 for chemo-sensitivity of ALL cells. Clin Cancer Res 17: 7605–7613.

Ehrhardt H, Höfig I, Wachter F, Obexer P, Fulda S, Terziyska N *et al.* (2012). NOXA as critical mediator for drug combinations in polychemotherapy. Cell Death Dis 3: e327.

Ewald JA, Desotelle JA, Wilding G, Jarrard DF (2010). Therapy-induced senescence in cancer. J Natl Cancer Inst 102: 1536–1546.

Frei E (1985). Curative cancer chemotherapy. Cancer Res 45: 6523–6537.

Jänicke RU, Engels IH, Dunkern T, Kaina B, Schulze-Osthoff K, Porter AG (2001). Ionizing radiation but not anticancer drugs causes cell cycle arrest and failure to activate the mitochondrial death pathway in MCF-7 breast cancer cells. Oncogene 20: 5043–5053.

Kaspers GJL, Veerman AJP, Pieters R, van Zantwijk I, Hählen K, van Wering ER (1995). Drug combination testing in acute lymphoblastic leukemia using the MTT assay. Leuk Res 19: 175–181.

Kawamura KI, Grabowski D, Weizer K, Bukowski R, Ganapathi R (1996). Modulation of vinblastine cytotoxicity by dilantin (phenytoin) or the protein phosphatase inhibitor okadaic acid involves the potentiation of anti-mitotic effects and induction of apoptosis in human tumour cells. Br J Cancer 73: 183–188.

Kilkenny C, Browne W, Cuthill IC, Emerson M, Altman DG (2010). NC3Rs Reporting Guidelines Working Group. Br J Pharmacol 160: 1577–1579.

Klier M, Anastasov N, Hermann A, Meindl T, Angermeier D, Raffeld M *et al.* (2008). Specific lentiviral shRNA-mediated knockdown of cyclin D1 in mantle cell lymphoma has minimal effects on cell survival and reveals a regulatory circuit with cyclin D2. Leukemia 22: 2097–2105.

Li T, Ling YH, Goldman ID, Perez-Soler R (2007). Schedule-dependent cytotoxic synergism of pemetrexed and erlotinib in human non-small cell lung cancer cells. Clin Cancer Res 13: 3413–3422.

Ling YH, el-Naggar AK, Priebe W, Perez-Soler R (1996). Cell cycle-dependent cytotoxicity, G2/M phase arrest, and disruption of p34cdc2/cyclin B1 activity induced by doxorubicinin synchronized P388 cells. Mol Pharmacol 49: 832–841.

Mattern J, Büchler MW, Herr I (2007). Cell cycle arrest by glucocorticoids may protect normal tissue and solid tumors from cancer therapy. Cancer Biol Ther 6: 1345–1354.

Mayer LD, Janoff AS (2007). Optimizing combination chemotherapy by controlling drug ratios. Mol Interv 7: 216–223.

McGrath J, Drummond G, McLachlan E, Kilkenny C, Wainwright C (2010). Guidelines for reporting experiments involving animals: the ARRIVE guidelines. Br J Pharmacol 160: 1573–1576.

Mollinedo F, Gajate C (2003). Microtubules, microtubule-interfering agents and apoptosis. Apoptosis 8: 413–450.

Müller HJ, Boos J (1998). Use of L-asparaginase in childhood ALL. Crit Rev Oncol Hematol 28: 97–113.

Nicoletti I, Migliorati G, Pagliacci MC, Grignani F, Riccardi C (1991). A rapid and simple method for measuring thymocyte apoptosis by propidium iodide staining and flow cytometry. J Immunol Methods 139: 271–279.

Petitjean A, Mathe E, Kato S, Ishioka C, Tavtigian SV, Hainaut P *et al.* (2007). Impact of mutant p53 functional properties on TP53 mutation patterns and tumor phenotype: lessons from recent developments in the IARC TP53 database. Hum Mutat 28: 622–629.

Ramaswamy S (2007). Rational design of cancer-drug combinations. N Engl J Med 357: 299–300.

Resnick-Silverman L, Manfredi J (2006). Gene-specific mechanisms of p53 transcriptional control and prospects for cancer therapy. J Cell Biochem 99: 679–689.

Rixe O, Fojo T (2007). Is cell death a critical end point for anticancer therapies or is cytostasis sufficient? Clin Cancer Res 13: 7280–7287.

Rozan LM, El-Deiry WS (2007). p53 downstream target genes and tumor suppression: a classical view in evolution. Cell Death Differ 14: 3–9.

Suzuki K, Matsubara H (2011). Recent advances in p53 research and cancer treatment. J Biomed Biotechnol 2011: 978312.

Webb JL (1963). Effect of more than one inhibitor. In: Hochster RM, Quastel JH (eds). Enzyme and Metabolic Inhibitors, Vol. 1. Academic Press: New York, pp. 487–512.

Yu J, Zhang L (2005). The transcriptional targets of p53 in apoptosis control. Biochem Biophys Res Commun 331: 851–858.

Yuan J, Krämer A, Matthess Y, Yan R, Spänkuch B, Gätje R *et al.* (2006). Stable gene silencing of cyclin B1 in tumor cells increases susceptibility to taxol and leads to growth arrest in vivo. Oncogene 25: 1753–1762.

Zhou BB, Elledge SJ (2000). The DNA damage response: putting checkpoints in perspective. Nature 408: 433–439.

Supporting information

Additional Supporting Information may be found in the online version of this article at the publisher's web-site:

Figure S1 Negative interaction between anthracyclines and vinca alkaloids in tumour cell lines. (A) SHEP cells were stimulated with doxo and VCR as in Figure 3A for time periods indicated. (B) Doxorubicin dose–response evaluated in SHEP cells. Alternatively, cells were pretreated with zVAD (50 μM) for 6 h before the addition of VCR. (C–E) Epithelial (C), mesenchymal (D) and neuroectodermal (E) tumour cell lines were simultaneously stimulated with doxo (100 ng·mL^{-1}) and VCR (300 ng·mL^{-1}) as in Figure 3A. Depicted is the expected apoptosis induction calculated by the fractional product as described in Methods and the measured apoptosis after combined stimulation displaying synergistic and antagonistic effects as summarized in Figure 3F. The concentrations of doxo and VCR, measurement of apoptosis, presentation of data and statistical analysis were performed as described in Figure 3 unless otherwise stated. *P < 0.05, ANOVA. NS = not significant.

Figure S2 Intracellular signal activation by doxo and VCR. (A–C) Western blot of total cellular protein was performed on SHEP cells stimulated with doxo and VCR as in Figure 3A. α-tubulin served as a loading control. Casp = Caspase, co = unstimulated control cells, cl. = cleaved, d = doxo, p = phosphorylated, h = hour, V = VCR. (D) SHEP cells were transiently transfected with plasmids containing survivin-GFP fusion protein (survivin), control GFP plasmid (mock) or left untreated (parental). Twenty-four hours later, cells were stimulated with doxo and VCR and evaluated as in Figure 3A. (E) SHEP cells from Supplemental Figure 2D were analysed for the cell cycle distribution using propidium iodide (upper panel) and discrimination of G2 and M phase by p-Histon H3 (lower panel) staining. Concentrations of doxo and VCR, measurement of apoptosis, Western Blot, presentation of data and statistical analysis were performed as described in Figures 1 and 3. *$P < 0.05$, ANOVA.

Figure S3 Central role of p53 in the inhibition of VCR induced apoptosis by doxo. HCT116 cells with wild-type p53 ($p53^{+/+}$), or somatic knock-out of p53 ($p53^{-/-}$) were stimulated for 72 h as in Figure 3A. Concentrations of doxo and VCR, measurement of apoptosis, Western Blot, presentation of data and statistical analysis were performed as described in Figures 1 and 3. *$P < 0.05$, ANOVA.

Figure S4 Combining doxo with VCR reduced life expectancy in mice compared with VCR treatment alone. A preclinical xenograft trial was performed using CEM leukaemia cells s.c. implanted into NSG mice; mice were treated with doxo (0.3 mg kg^{-1}) and/or VCR (0.9 mg kg^{-1}) or placebo once weekly in week 1 and 2; animals were killed whenever tumour volume exceeded a defined threshold. Tumour sizes were published in Ehrhardt *et al.*, 2011a (for experimental details, see there); here, survival times of mice are shown for the different treatment groups.

Figure S5 Identical signalling mechanisms in A498 renal cancer cells. (A) See Figure 1A. (B–E). See Figures 2, 3A and B. (F,G). See Supplementary Figure 1A and B. (H–M) See Figure 3D and E and Figure 4A–C. (N–Q). See Supporting Information Figure S2. (R–V). See Figure 5A–D and Figure 6A.